Available online at www.sciencedirect.com
ScienceDirect
Journal of the European Ceramic Society 30 (2010) 3351–3356
www.elsevier.com/locate/jeurceramsoc

Carbon nanotube/boehmite-derived alumina ceramics obtained by hydrothermal synthesis and spark plasma sintering (SPS)

Ali Can Zaman [a], Cem B. Üstündağ [a,b], Ali Çelik [c], Alpagut Kara [c], Figen Kaya [d], Cengiz Kaya [a,*]

[a] *Department of Metallurgical and Materials Engineering, Yildiz Technical University, Davutpasa Campus, Esenler, Istanbul, Turkey*
[b] *Vocational School, Department of Ceramics, Yildiz Technical University, Maslak Campus, Maslak, İstanbul, Turkey*
[c] *Department of Materials Science and Engineering, Anadolu University, Eskişehi, Turkey*
[d] *Department of Metallurgical Engineering, Zonguldak Karaelmas University, Zonguldak, Turkey*

Received 10 June 2010; received in revised form 30 June 2010; accepted 20 July 2010
Available online 21 August 2010

Abstract

Preparation, structure and properties of hydrothermally treated carbon nanotube/boehmite (CNT/γ-AlOOH) and densification with spark plasma sintering of Al_2O_3 and CNT/Al_2O_3 nanocomposites were investigated. Hydrothermal synthesis was employed to produce CNT/boehmite from an aluminum acetate ($Al(OH)(C_2H_3O_2)_2$) and multiwall-CNTs mixture (200 °C/2 h.). TEM observations revealed that the size of the cubic shape boehmite particles lies around 40 nm and the presence of the interaction between surface functionalized CNTs and boehmite particles acts to form 'nanocomposite particles'. Al_2O_3 and CNT/Al_2O_3 compact bodies were formed by means of spark plasma sintering (SPS) at 1600 °C for 5 min using an applied pressure of 50MPa resulting in the formation of stable α-Al_2O_3 phase and CNT–alumina compacts with nearly full density. It was also found that CNTs tend to locate along the alumina grain boundaries and therefore inhibit the grain coarsening and cause inter-granular fracture mode. The DC conductivity measurements reveal that the DC conductivity of CNT/Al_2O_3 is 10^{-4} S/m which indicate that there is a 4 orders of magnitude increase in conductivity compared to monolithic Al_2O_3. The results of the microhardness tests indicate a slight increase in hardness for CNT/Al_2O_3 (28.35 GPa for Al_2O_3 and 28.57 GPa for CNT/Al_2O_3).

Keywords: Al_2O_3; Carbon nanotube; Hydrothermal synthesis; Spark plasma sintering

1. Introduction

Graphite has C–C sp^2 bonds which are stronger than the C–C sp^3 bonds in diamond (the hardest known material) because the C–C sp^2 bond length is shorter than the C–C sp^3.[1] However, the molecular forces between the graphite layers are van der Waals forces, which allow them to slide easily.[1] CNTs are rolled up sheets of graphite, they consist of one or more cylindrical walls, having distinctive features, such as high tensile strength in the range of 60 GPa,[2] rigidity up to 1.8 TPa[3] and electrical conductivity of the order of 1.85×10^3 S/cm[4] for multi walled carbon nanotubes (MWCNTs). Due to the unique features of the CNTs, there are many possible applications for CNTs including nanocomposites. To create functional CNT-reinforced composites, two main problems have to be overcome: (i) homogeneous dispersion of nanotubes in the matrix and (ii) generation of strong interfacial bonding between CNTs and the matrix. CNTs can be considered to be long flexible nano-fibers which can entangle very easily with each other[1] and they form aggregates easily because of the van der Waals attractive forces. In agglomerated state, CNTs resemble graphite because the van der Waals forces dominate, therefore they can easily slide when subjected to an applied stress. This situation degrades the mechanical properties of CNT nanocomposites. Large scale industrial production of CNT based materials is due to their remarkable electrical properties.[5] The increase in the conductivity of an insulating material, such as alumina depends on the concentration and the aspect ratio of the conductive filler.[6] The conductivity increases with the increasing filler content and above a critical concentration, the fillers tend to link to each other to form conductive pathways across the insulating matrix[6] and therefore conductivity of the composite increases dramatically with increasing filler content. Fiber shape fillers are preferential for reinforcing ceramics to increase the electrical conductivity, because the

* Corresponding author.
E-mail address: cngzky@yahoo.co.uk (C. Kaya).

0955-2219/$ – see front matter © 2010 Elsevier Ltd. All rights reserved.
doi:10.1016/j.jeurceramsoc.2010.07.037

incorporation volume of the second phase into the insulating matrix can be reasonably low. At low filler content the composite can transform into a conductor, yet retains its mechanical properties.

The dispersion problems of CNTs arise at higher filler contents which degrades the mechanical properties. Particulates, whiskers and fiber shape fillers can be used to improve the toughness of the ceramics, but the reinforcing effect of fibers (such as CNTs) is higher than for the others.[6–11] The reinforcements can be made of ceramics or metals[6] but ceramics are ideal as metal fiber reinforcements show relatively low thermal capability and poor chemical resistance which limits the application temperature and environment.[12] Besides, generally greater toughness, strength and hardness values are achieved in fine grained materials therefore CNTs were proved to be suitable grain refiners.[13] In conclusion, CNTs can be considered to be suitable reinforcements to increase the mechanical properties as well as the electrical conductivity of alumina.

The common approaches to make CNT nanocomposites are CVD technique and colloidal processing. In CVD technique, CNTs are grown using metal catalyst particles positioned on ceramic substrates. The remaining catalyst particles, residual amorphous carbon and entangled CNTs in the ceramic matrix can lead to degradation of the properties of the composite.[13,14] In colloidal processing, CNTs and alumina dispersed in solvents with surfactant additions are dried and thermally treated.[15] There are some positive results for CNT/reinforced alumina nanocomposites in terms of mechanical properties[13,16,17] and electrical conductivity.[15,18] However, homogeneous dispersion of nanotubes in the matrix still remains a serious problem which pushes researchers to find new approaches.

Carbon nanotubes tend to be in a state of an entangled mass because of their flexible fiber-like structure and also the consequence of the strong attractive forces between them. This makes the dispersion process a compelling crucial factor in obtaining functional CNT-reinforced composites. Before mixing of CNTs and ceramic powders, carbon nanotubes have to be functionalized for the homogeneous dispersion. The generally implemented method includes the acid treatment which induces defects on the nanotubes.[19] Therefore acid treated CNTs possess limited strength and conductivity. But, hydrothermal synthesis can provide an environment for nanotubes to be functionalized while giving little or no harm, unlike acid treatment.[20] Because the high temperatures and pressures may break the hard big agglomerates of CNTs and force functional groups (COOH, OH) to attach on the sidewalls and open ends of CNTs under the presence of appropriate chemicals, repulsion between individual tubes can be maintained during hydrothermal synthesis.

In this study, CNT/boehmite nanocomposite powders were synthesized by hydrothermal synthesis from a mixture of aluminum acetate and MWCNTs in aqueous medium. Densification of the powders was achieved by means of SPS. CNT/boehmite and CNT/Al_2O_3 were both characterized by TEM. XRD analysis, SEM observations, DC conductivity measurements (2 point probe technique); hardness tests were also conducted for both monolithic Al_2O_3 and CNT/Al_2O_3.

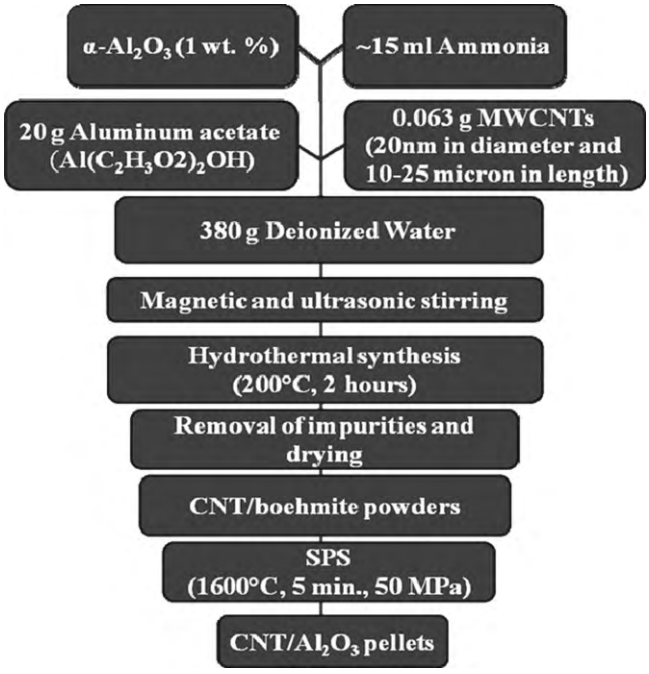

Fig. 1. Manufacturing process for the CNTs-reinforced Al_2O_3 nanocomposites.

2. Experimental details

Multi walled carbon nanotubes (20 nm in diameter and 10–25 μm in length, Thomas Swan Co. Ltd., UK), aluminum acetate basic (Al(OH)($C_2H_3O_2$)$_2$, Sigma Aldrich), ammonia (Merck, 25%) and α-Al_2O_3 (Tai Macron, DM-DR, Japan) were used as starting materials in this study.

To obtain 1 wt.% CNT-reinforced boehmite, the solution of aluminum acetate and MWCNTs was prepared in water in the weight of approximately 400 g for each synthesis. 0.063 g MWCNTs, 20 g aluminum acetate and ~15 ml ammonia and α-Al_2O_3 as seeding material (0.1 wt.% of the aluminum acetate) were mixed in 380 g distilled water. A solution without CNT content was also prepared for the production of pure boehmite and for the sake of comparison the synthesis conditions were kept identical to the CNT/boehmite production. The pH of the suspension was initially 4 but it was increased to 9 by the addition of ammonia. The obtained solutions were ultrasonicated until the color of the solution turned into dark grey and until there were no visible black agglomerates in the suspension. Hydrothermal synthesis was performed at 200 °C for 2 h in a high pressure autoclave having 500 ml Teflon lined reaction chamber (Berghoff Br-300, Germany). The pressure of the synthesis was 1 MPa. Finally, CNT-reinforced boehmite matrix nanocomposite and boehmite solutions were obtained. The water soluble impurities were extracted by removing the water above the settled solutions till the pH decreased to 7. After drying in an oven at 100 °C the mixture was sieved. The obtained grey powders (The color of the boehmite powders were white.) were spark plasma sintered (FCT system HP D25/1) at 1600 °C under a pressure of 50 MPa in vacuum for 5 min (see Fig. 1). The resultant samples had dimensions of 20 mm in diameter and 5 mm in thickness.

SEM and TEM observations were used to characterize the interaction between the CNTs and the AlOOH and Al_2O_3 matrices. The DC electrical conductivities were measured using 2 point probe technique. The hardness measurements were obtained by a micro-vickers hardness tester. Density measurements were recorded using Archimedes technique.

3. Results and discussions

Under hydrothermal conditions aluminum acetate undergoes a decomposition to form acetic acid (CH_3COOH) and boehmite (γ-AlOOH). The aluminum acetate decomposes according to the following reaction under hydrothermal conditions (Eq. (1)):

$$Al(OH)(C_2H_3O_2)_2 + H_2O \rightarrow (\gamma\text{-AlOOH}) + 2CH_3COOH \quad (1)$$

Carboxylic acid (COOH) and hydroxyl (OH) groups can attach on the surface or open ends of CNTs during the hydrothermal synthesis which effectively results in the functionalization of the CNTs. The hydrothermally synthesized stable sols containing pure boehmite and CNTs/boehmite mixture are shown in Fig. 2a and b, respectively. Although the different densities of carbon nanotubes (2.1 g/cm^3) and boehmite (3.04 g/cm^3) may be expected to favor the phase segregation, that event is not seen even though the sols are kept for a couple of days.

When heating up boehmite, transitional alumina phases are formed. The sequence of the phases occurred during the thermal treatment is γ, δ, θ and finally α-alumina.[21] Additionally, large amount of dehydration occur and these events result in the formation of porosity within the structure under relatively low pressures during thermal treatment. By means of implementation of high pressures in SPS, the formation of the porosity can be inhibited and furthermore, SPS provides the ceramic powders to be sintered quickly and enable the fabrication of relatively fine grained materials.

TEM analysis of CNT/boehmite was performed in order to assess the degree of the interaction between nanotubes and boehmite matrix and also to determine the particle size and morphology of the boehmite crystals, as shown in Fig. 3. Fig. 3a shows the boehmite crystals to be near cube or hexagonal shapes with a length of 30–40 nm. Fig. 3b shows the TEM image of MWCNTs-boehmite composite particles indicating that MWCNT is covered with boehmite particles, which is the evidence of the attraction between the CNTs and boehmite matrix as a result of good surface functionalization of CNT surfaces.

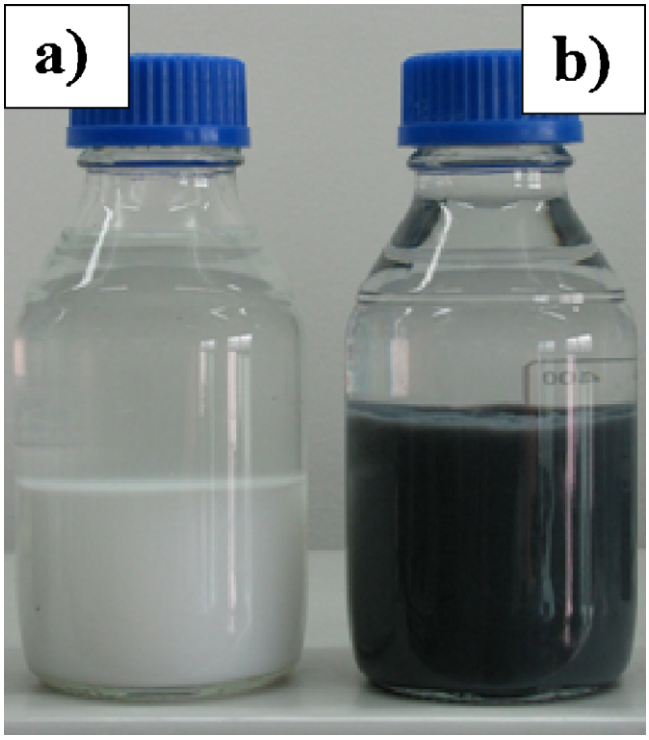

Fig. 2. Hydrothermally synthesized boehmite (a) and CNT/boehmite sols (b) indicating the presence of stable suspensions and the absence of phase segregation in CNT–boehmite mixture (b).

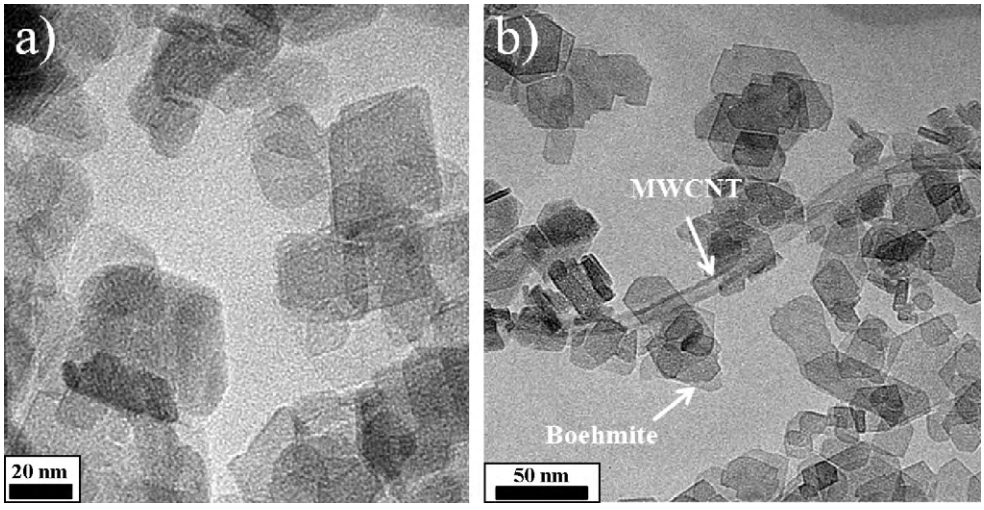

Fig. 3. TEM pictures of hydrothermally synthesized cubic/hexagonal shape boehmite crystals with a length of 30–40 nm (a) and CNT/boehmite mixture indicating the good coverage of CNTs by boehmite particles (b).

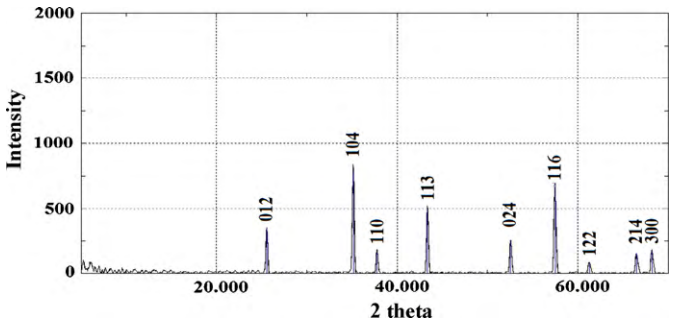

Fig. 4. XRD pattern of boehmite-derived Al_2O_3 after SPS indicating that there is no other phase present (α-Al_2O_3: JCPDS file no: 43-1484).

The sieved powder samples were sintered with SPS at 1600 °C for 5 min under a pressure of 50 MPa. XRD analysis of pellets was revealed that all the peaks match the standard peaks of α-Al_2O_3 with no other transitional aluminas, as shown in Fig. 4. This is a significant finding that shows boehmite-derived α-alumina can be obtained in a very short time (5 min) using SPS proving that temperature and pressure speeds up the transformation process of boehmite to alumina (even if it is seeded, boehmite needs 2–4 h to complete the transformation reactions during pressureless sintering at about 1500–1600 °C). There is no residual peak that indicates the presence of other impurities as shown in Fig. 4.

In order to determine the effects of CNT addition on the fracture behavior and microstructure of alumina, SEM observations were conducted on spark plasma sintered samples, as shown in Fig. 5. The two SEM micrographs of fractured surfaces of boehmite-derived α-Al_2O_3 in different magnifications show the fracture mode of alumina to be mixed mode (inter-granular and trans-granular fracture), as shown in Fig. 5a and b. It is also seen from Fig. 5a and b that the grain size of Al_2O_3 is around 2.5 μm. However, the fractured surface of the CNT/Al_2O_3 shows dominantly inter-granular mode of fracture, as shown in Fig. 5c and d. Fig. 5c and d also shows that the size of Al_2O_3 grains is approximately 1 μm in CNT/Al_2O_3. The change in fracture mode of alumina from mixed mode to inter-granular fracture with the addition of CNTs is caused by the location of the CNTs along the grain boundaries of Al_2O_3, as shown in Fig. 5c and d. This also explains why the grain size of alumina (1 μm) in CNT/alumina samples is much smaller than that of monolithic alumina (2.5 μm) as the CNTs prevent grain growth during SPS, as shown in Fig. 5c and d. The high magnification micrograph of CNT/ Al_2O_3 in Fig. 5d clearly shows the tendency of MWCNTs to locate between Al_2O_3 grains.

TEM micrographs of SPSed boehmite-derived pure α-Al_2O_3 and CNT/Al_2O_3 are shown in Fig. 6. The TEM micrographs of alumina shown in Fig. 6a indicate the dense structure after sintering and also the presence of some intra-granular pores (Fig. 6a). It is also seen in Fig. 6b that the grain size of CNT/Al_2O_3 is about 1 μm which is in a good agreement with the SEM results shown in Fig. 5. It should also be noted from Fig. 6a that the grain boundary of alumina is very clear proving the absence of any undesired phases. The TEM micrographs of CNT-reinforced alumina samples are also shown in Fig. 6 c and d. The location of the CNTs along the alumina grain boundaries is determined in Fig. 6c and d which is considered to be responsible for the finer alumina grain size (1 μm) in the CNT–alumina samples. Fig. 6 clearly shows the grain refinement effect of the CNT addition which also explains the inter-granular fracture mode of CNT–alumina samples. The micrograph that focuses on the grain boundaries reveals the presence of the MWCNTs between

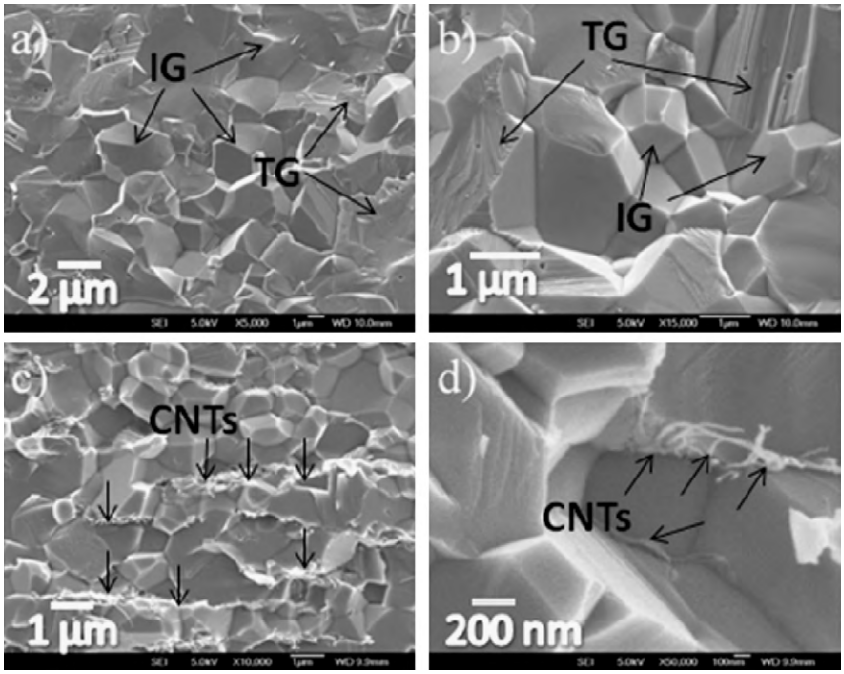

Fig. 5. SEM images of fractured surface of monolithic α-Al_2O_3 (a and b) and CNT–alumina samples (c and d) indicating the presence of mixed mode of fracture for pure alumina (a and b) and inter-granular fracture in CNT–alumina samples (c and d). TG: trans-granular farcture and IG: inter-granular fracture.

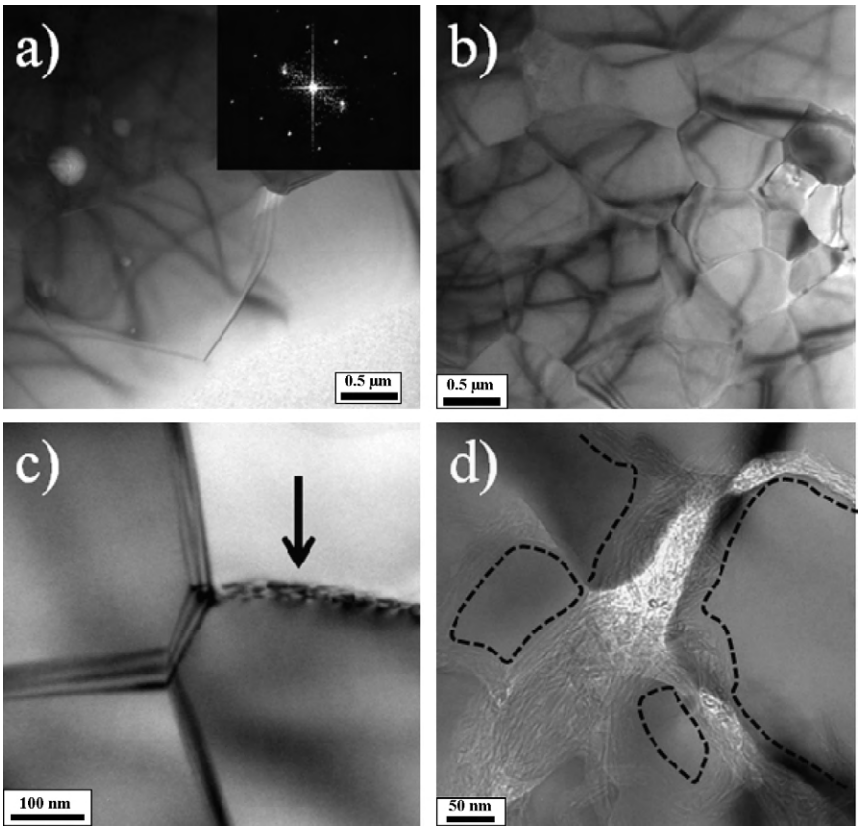

Fig. 6. TEM micrograph of boehmite-derived Al_2O_3 (a) and CNT/Al_2O_3 samples (b–d). It is clearly seen in the high magnification micrograph in (d) that CNTs are formed a conductive and continuous network along the alumina grain boundaries.

the alumina grains (actually most of them are aligned along the long axis of the grain boundaries, as shown in Fig. 6d)) as indicated by an arrow in Fig. 6c.

The processing conditions, densities, conductivity and hardness measurements of the Al_2O_3 and CNT/Al_2O_3 nanocomposite studied are given in Table 1. The DC conductivities of the samples are 10^{-8} S/m and 10^{-4} S/m for Al_2O_3 and CNT/Al_2O_3, respectively which indicates a significant increase in conductivity due to the presence of CNTs within alumina structure (see also Fig. 6c), as shown in Table 1.

The densities are 3.88 g/cm^3 and 3.95 g/cm^3 for monolithic alumina and CNT/alumina, respectively, as shown in Table 1. The theoretical densities of MWCNTs are taken 2.1 g/cm^3 and 3.97 g/cm^3 for Al_2O_3. Considering these values, the relative densities are 98% and 99.9% for the CNT/Al_2O_3 (1 wt.%, 1.87 vol.%) and Al_2O_3, respectively. The difference in the densities of the products reveals the existence of a certain amount of CNT agglomeration within the alumina matrix but overall it does not create a significant difference.

The hardness of CNT/Al_2O_3 and Al_2O_3 are 28.57 GPa and 28.35 GPa, respectively. The slight increase in the hardness can be the consequence of the grain refinement effect of MWCNTs in alumina. However, further studies are currently underway to see the relationships between grain size and hardness.

In conclusion, the results presented in Figs. 3–6 and Table 1 indicate that CNT-reinforced alumina based ceramics with nearly full density are achievable if some critical issues are resolved before using spark plasma sintering. First of all, the surface functionalization of CNTs which results in the formation of homogeneously mixed and stable boehmite and CNT–boehmite suspensions should be provided by a method which does not harm CNTs (as far as the authors are aware, for the first time to date, the surface functionalization of CNTs are achieved by hydrothermal process which has no harmful effect on CNTs). If the CNTs are distributed within the alumina structure, fine grained sintered alumina with high conductivity is achieved by the location of CNTs along the alumina grain boundaries. Now, further studies are underway to explore mechanical properties of CNT–alumina and their relationships

Table 1
Summary of the synthesis conditions and obtained values for synthesized products (note: TD denotes the theoretical density of Al_2O_3 and SPS denotes spark plasma sintering).

Composition	SPS parameters	Grain size (μm)	Density (%TD)	Hardness (GPa)	DC conductivity (S/m)
Boehmite-derived α-Al_2O_3	1600 °C/5 min 50 MPa	2.5	99.9	28.35	10^{-8}
Boehmite-derived CNT/Al_2O_3 (1 wt.%, 1.87 vol.%)	1600 °C/5 min 50 MPa	1	98	28.57	10^{-4}

with microstructure in terms of grain size, CNT content and porosity.

4. Conclusion

CNT/boehmite nanocomposite powders were synthesized by means of hydrothermal synthesis (200 °C/2 h) which also provides the necessary compound for surface functionalization of CNTs and formation of boehmite particles with a particle size of 40 nm. The densification of CNT/boehmite and boehmite powders was maintained by means of SPS at 1600 °C for 5 min under 50 MPa (it is also found that boehmite can be transformed to stable α-alumina in 5 min under these conditions. TEM and SEM analysis of CNT/Al_2O_3 shows that CNTs inhibit grain coarsening and the addition of 1 wt.% CNTs to alumina decreases the grain size of Al_2O_3 from around 2.5 μm to 1 μm. It is also shown that CNTs tend to locate along the alumina grain boundaries which inhibits alumina grain growth during sintering. The location of CNTs along the grain boundaries are also responsible for inter-granular fracture mode of CNT–alumina samples whilst the fracture mode of monolithic alumina is mixed (trans- and inter-granular fracture). Relative densities are measured to be 99.9% for Al_2O_3 and 98% for CNT/Al_2O_3. The DC conductivities of SPSed products show 4 orders of magnitude increase (10^{-8} S/m for Al_2O_3 and 10^{-4} S/m for CNT/Al_2O_3) in CNT/ Al_2O_3 (with the addition of 1 wt.% CNTs) over monolithic alumina. CNT/Al_2O_3 ceramics are considered to be suitable for some application areas that are demanding high temperature capability to increase efficiency and reduction of weight, if the protection against oxidation is maintained. In addition the higher electrical conductivity provides higher thermal conductivity for the Al_2O_3 matrix; this can give them good thermal shock resistance which is a required property for high temperature applications.

Acknowledgements

This work was funded by TUBITAK (The Scientific and Technological Research Council of Turkey) under the contract number 108T651. Prof. Gültekin Göller from Istanbul Technical University and Özgür Duygulu from TUBITAK MAM are also acknowledged for the assistance with FEG-SEM and TEM studies, respectively.

References

1. Advani SG. *Processing and properties of nanocomposites*. NJ: World Scientific; 2007.
2. Yu MF, Lourie O, Dyer MJ, Moloni K, Kelly TF, Ruoff RS. Strength and breaking mechanism of multiwalled carbon nanotubes under tensile load. *Science* 2000;**287**:637–40.
3. Treacy MM, Ebbesen TW, Gibson JM. Exceptionally high Young's modulus observed for individual carbon nanotubes. *Nature* 1996;**381**:678–80.
4. Ando Y, Zhao X, Shimoyama H, Sakai G, Kaneto K. Physical properties of multiwalled carbon nanotubes. *Int J Inorg Mater* 1999;**1**(1):77–82.
5. Vaisman L, Wagner HD, Marom G. The role of surfactants in dispersion of carbon nanotubes. *Adv Colloid Interface* 2006;**128–130**:37–46.
6. Tjong SC. *Carbon naotube reinforced composites: metal and ceramic matrices*. Weinheim: Wiley-VCH; 2009.
7. Knowles KM, Turan S. Boron nitride-silicon carbide interphase boundaries in silicon nitride-silicon carbide particulate composites. *J Eur Ceram Soc* 2002;**22**:1587–600.
8. Liu YS, Cheng L, Zhang L, Hua Y, Yang W. Microstructure and properties of particle reinforced silicon and silicon nitride ceramic matrix composites prepared by chemical vapor infiltration. *Mater Sci Eng A* 2008;**475**:217–23.
9. Hua Y, Zhang L, Cheng L, Wang J. Silicon carbide whisker reinforced silicon carbide composites by chemical vapor infiltration. *Mater Sci Eng A* 2006;**428**:346–50.
10. Park K, Vasilos T. Interface and thermal shock resistance of SiC fiber/SiC composites. *Scr Mater* 1998;**39**:1593–8.
11. Zhu S, Mizuno M, Kagawa Y, Mutoh Y. Monotonic tension, fatigue and creep behavior of SiC-fiber reinforced SiC-matrix composites: a review. *Mater Sci Eng A* 1999;**59**:833–51.
12. Boccaccini AR. Continuous fibre reinforced glass and glass-ceramic matrix composites. In: Bansal NP, editor. *Handbook of ceramic composites*. Boston: Kluwer Academic Publishers; 2005. p. 469.
13. Zhang SC, Fahrenholtz WG, Hilmas GE, Yadlowsky EJ. Pressureless sintering of carbon nanotube–Al_2O_3 composites. *J Eur Ceram Soc* 2010;**30**:1373–80.
14. Flahaut E, Peighey A, Laurent C, Marliere C, Chastel F, Rousset A. Carbon nanotube metal–oxide nanocomposites: microstructure, electrical conductivity and mechanical properties. *Acta Mater* 2000;**48**:3803–12.
15. Poorteman M, Traianidis M, Bister G, Cambier F. Colloidal processing, hot pressing and characterisation of electroconductive MWCNT-alumina composites with compositions near the percolation threshold. *J Eur Ceram Soc* 2009;**29**:669–75.
16. Zhang T, Kumari L, Du GH, Li WZ, Wang QW, Balani K, et al. Mechanical properties of carbon nanotube–alumina nanocomposites synthesized by chemical vapor deposition and spark plasma sintering. *Composites A* 2009;**40**:86–93.
17. Ahmad I, Cao H, Chen H, Zhao H, Kennedy A, Zhu YQ. Carbon nanotube toughened aluminium oxide nanocomposite. *J Eur Ceram Soc* 2009;**30**:865–73.
18. Inam F, Yan H, Jayaseelan DD, Peijs T, Reece M. Electrically conductive alumina–carbon nanocomposites prepared by spark plasma sintering. *J Eur Ceram Soc* 2010;**30**:153–7.
19. Yamamoto G, Omori M, Hashida T, Kimura H. A novel structure for carbon nanotube reinforced alumina composites with improved mechanical properties. *Nanotechnology* 2008;**19**:315708–15.
20. Zaman AC, Ustundag CB, Kaya C. Boehmite derived surface functionalized carbon nanotube-reinforced macroporous alumina ceramics. *J Eur Ceram Soc* 2010;**30**:2525–31.
21. Levin I, Brandon D. Metastable alumina polymophs: crystal structures and transition sequences. *J Am Ceram Soc* 1998;**81**:1995–2012.